Canadian Journal of Chemistry
Published by
THE NATIONAL RESEARCH COUNCIL OF CANADA

Journal canadien de chimie
Publié par
LE CONSEIL NATIONAL DE RECHERCHES DU CANADA

Volume 58 Number 17 September 1, 1980

Volume 58 numéro 17 1 septembre 1980

Kinetics of the magnetite–maghemite–hematite transformation, with special reference to hydrothermal systems

THOMAS WILSON SWADDLE[1] AND PHILLIP OLTMANN
Department of Chemistry, The University of Calgary, Calgary, Alta., Canada T2N 1N4

Received January 23, 1980

THOMAS WILSON SWADDLE and PHILLIP OLTMANN. Can. J. Chem. **58**, 1763 (1980).

Maghemite, prepared in the usual way (but with exclusion of silica, e.g., from glassware) by precipitation of non-stoichiometric magnetite $Fe_{3-x}O_{4-x}$ in aqueous MOH (M = Na, K) followed by air oxidation, picks up moisture from the air to reach the limiting composition $M_{\delta}H_{1-\delta}Fe_5O_8$, where $\delta \sim 0.02$–0.03 for fresh material, but changes under hydrothermal conditions because of ion exchange. Despite the role of absorbed moisture in stabilizing maghemite, formation of the latter from $Fe_{3-x}O_{4-x}$ is markedly retarded, and its decomposition to α-Fe_2O_3 greatly accelerated, under hydrothermal conditions relative to the rates of the corresponding reactions of the dry solids. The rate of hydrothermal decomposition of maghemite is strongly retarded by silica. Over the range 160–187°C at least, silica-free maghemite decomposes in water according to the empirical equation $-\ln(1-\alpha) = (kt)^n$, where α is the fractional extent of decomposition, and $n \sim 2.5$ for neutral water (with $k = 1.3 \times 10^{-5}\ s^{-1}$ at 160°C and $3.1 \times 10^{-5}\ s^{-1}$ at 175°C) but approaches unity, without major effects on the overall time-scale of reaction, at high [MOH]. The mechanistic significance of these and previous results are considered; the hydrothermal conversion of maghemite to hematite evidently proceeds by a dissolution–reprecipitation sequence.

THOMAS WILSON SWADDLE et PHILLIP OLTMANN. Can. J. Chem. **58**, 1763 (1980).

La maghémite, préparée de manière habituelle (mais avec élimination de la silice par exemple celle de la verrerie) par précipitation de la magnétite non stoechiométrique $Fe_{3-x}O_{4-x}$ dans du MOH aqueux (M = Na, K) suivie d'une oxydation à l'air, absorbe l'humidité de l'air pour atteindre une composition limite de $M_{\delta}H_{1-\delta}Fe_5O_8$ où $\delta \sim 0.02$–0.03 pour le produit frais, mais il se produit des changements dans des conditions hydrothermiques par suite de l'échange d'ions. En dépit du rôle de l'humidité absorbée en tant que stabilisatrice de la maghemite, la formation de cette dernière à partir de $Fe_{3-x}O_{4-x}$ est fortement retardée et sa décomposition en Fe_2O_3 α est grandement accélérée dans des conditions hydrothermiques s'apparentant aux vitesses des réactions correspondantes des solides secs. La vitesse de décomposition hydrothermique de la maghémite est fortement retardée par la silice. Au moins dans l'intervalle de 160–187°C, la maghémite dépourvue de silice se décompose dans l'eau selon l'équation empirique $\ln(1-\alpha) = (kt)^n$, où α est le degré fracitonnel de décomposition et $n \sim 2.5$ pour l'eau neutre (avec $k = 1.3 \times 10^{-5}\ s^{-1}$ à 160°C et $3.1 \times 10^{-5}\ s^{-1}$ à 175°C) mais s'approche de l'unité sans effet appréciable sur le temps global de réaction à forte concentration de MOH. On considère la signification du point de vue du mécanisme de ces résultats et des résultats antérieures; la conversion hydrothermique de la maghémite en hématite se fait évidemment selon la séquence dissolution–reprécipitation.

[Traduit par le journal]

Introduction

The cubic iron(III) oxide maghemite ("γ-Fe_2O_3"), although thermodynamically unstable with respect to hematite (α-Fe_2O_3) and not usually considered a common mineral, does occur widely in terrestrial (notably highly-weathered tropical) soils (1, 2), has been reported to be an important secondary mineral in certain subvolcanic hydrothermal breccia bodies (3), appears to be a major constituent of the sands of Mars (4, 5), and has even been said to be the substance responsible for the visible absorption spectrum of interstellar matter (6), though the last seems improbable (7).

Maghemite forms in nature either through the oxidation of magnetite (Fe_3O_4) if this is sufficiently finely-divided (3, 8–15), through the oxidation at ambient temperatures of aqueous iron(II) via precipitated "green rusts" under conditions of limited O_2 supply (i.e., slow reaction) (16, 17), and possibly through dehydration of lepidocrocite (γ-FeO(OH)) (1, 18–20) although a redox cycle may be involved in this last case (1, 21). Whatever the mechanism, it appears that the presence of water is necessary for the formation of maghemite, natural or synthetic (7,

---

[1] To whom correspondence should be addressed.

0008-4042/80/171763-10$01.00/0

11, 22, 23), probably because the cation vacancies in the pseudo-spinel lattice can be stabilized by the occupation of some or all of the vacant octahedral cation sites by H^+ up to the limiting composition HFe_5O_8, i.e., $5Fe_2O_3 \cdot H_2O$ (24, 25), and indeed virtually all samples of maghemite seem to contain some bound water (11, 22–25). Yet, in spite of this, it has been shown (20, 26, 27) that water also facilitates the conversion of maghemite to α-Fe_2O_3.

A major objective of the present study was therefore to elucidate the kinetic factors governing the metastability of maghemite in aqueous (in effect, hydrothermal) environments. This has relevance to the understanding of the corrosion of ferrous metals in high-temperature aqueous environments; a film of maghemite is known to form in the anodic oxidation of iron in water at room temperature (28) and in the aqueous corrosion of pearlitic steel at pH 6.2–6.8 over the temperature range 20–287°C (29), as well as in the "dry" oxidation of iron by (moist) air near 20°C (30, 31). Maghemite may, in fact, be more common as a corrosion product than is generally appreciated, since the X-ray diffraction pattern of the poorly-crystalline material is difficult to distinguish from that of magnetite (30); this may have relevance, for example, to the characterization of the finely-divided corrosion products ("crud") formed in the heat-transfer systems of water-cooled nuclear power reactors, especially if there exists the possibility of an excursion to oxidizing conditions. In any event, we wish to stress once again (32) that the possible formation and persistence of metastable intermediates such as maghemite must be taken into account when making thermodynamically-based predictions about the outcome of hydrothermal reactions, since these substances could well be the actual reactive species governing the mechanism and course of reaction.

Experimental

Characterization of Materials

Solids in general were characterized by their powder X-ray diffraction (XRD) patterns in comparison with those in the JCPDS files. Elemental analyses, where required, were carried out on solutions of the solids in a small excess of 8–12 *M* HCl (*M* = mol dm^{-3} at 294 K and 89 kPa). Iron(II) was determined by titration with chromate(VI), and iron(III) both gravimetrically as tris(8-hydroxyquinolinato) iron(III) and volumetrically with chromate(VI) after $SnCl_2$ reduction, with good agreement (±0.2%) (33). The sodium and potassium contents of iron compounds were determined (±2%) by flame emission analysis, using a Varian Techtron Model 1200 spectrophotometer and KNO_3 and CsCl as the respective ionization suppressants.

Specific surface areas (SSA) were determined (± 2 m^2 g^{-1}) by the BET(N_2) method with a Micromeritics Model 2200 High-Speed Surface Area Analyzer, degassing the samples for 40 min at 180 ± 10°C under dry N_2.

Preparation of Materials

Except where the use of glassware is specifically indicated, the maghemite samples and reaction media referred to below were "silica-free", i.e., they were prepared using polyethylene or other non-siliceous laboratory ware exclusively. Fresh Fisher Certified analytical grade reagents were used; KOH was supplied in plastic bottles, and was therefore preferred over NaOH, which came in glass jars. Distilled water was passed through Barnstead deionizer and organic removal cartridges before use.

Magnetite

Finely-particulate "magnetite", conveniently described as a non-stoichiometric solid solution, $x\gamma$-$Fe_2O_3 \cdot (1 - x)Fe_3O_4$ or $Fe_{3-x}O_{4-x}$ exclusive of absorbed water, was typically prepared by slowly adding 1500 cm^3 of a solution of iron(II) sulfate (0.14 *M*) and iron(III) ammonium sulfate (0.28 *M*) to 500 cm^3 fresh aqueous KOH (6.4 *M*), maintained at 90–95°C with vigorous stirring throughout the addition. The black precipitate was filtered, washed thoroughly with water until the filtrate was neutral and then with acetone, air-dried, and powdered. This material was typically found to contain 14.5% iron(II) (cf. 24.1% for stoichiometric Fe_3O_4), i.e., x in $Fe_{3-x}O_{4-x}$ was 0.49, ignoring the small absorbed water content. Removal of O_2 from the reaction mixture by purging with N_2 increased the iron(II) content only marginally (to 15.1%), since most of the loss of iron(II) probably resulted from the spontaneous decomposition of $Fe(OH)_2$ (34, 35). The XRD patterns contained no reflections other than those of $Fe_{3-x}O_{4-x}$; in particular, no iron silicates were detectable even when the preparation was done in glassware (contrast the formation of nickel talc in $Ni(OH)_2$ preparations (32)). The specific surface area (SSA) of samples so prepared was typically 75 m^2 g^{-1}; larger SSA's (to 120 m^2 g^{-1}) were obtainable by more rapid mixing of the reagents and allowing the temperature to fall accordingly, while very slow mixing produced an SSA of about 45 m^2 g^{-1}.

Well-crystallized (SSA < 0.1 m^2 g^{-1}), stoichiometric magnetite was made by hydrothermal decomposition of $FeNTA \cdot H_2O$ (36). Yields of some 90% were obtained in 50–80 h at 240°C with initial concentrations Fe(III) ~ 0.1 *M*, NaOH ~ 0.3 *M*. With [FeNTA] ~ 0.2 *M*, well-crystallized $FeCO_3$ was also precipitated, while at 185–190°C the product was α-Fe_2O_3.

Maghemite

Finely-particulate magnetite was completely converted to maghemite by heating in air for 15 min at 180°C. At room temperature, the product picked up moisture rapidly from the air until a constant weight was reached. No crystalline phases other than maghemite could be detected by XRD in this final product, even after heating for a further 72 h in air at 180°C. A sample (**A**) of specific surface 72 m^2 g^{-1}, used in most of the kinetic experiments described below, analyzed as follows: Fe^{3+}, 68.0 ± 0.2%; Fe^{2+}, < 0.005; H_2O (weight loss on heating to 800°C), 2.1 ± 0.1; K^+, 0.279 ± 0.005; Na^+, < 0.005; $SO_4{}^{2-}$, undetectable. *Anal.* calcd. for $(K_{0.029}H_{0.971})Fe_5O_8$: Fe^{3+} 68.2, H_2O 2.20, K^+ 0.277.

A sample (**B**) of maghemite (SSA 76 m^2 g^{-1}) prepared using NaOH in place of KOH analyzed similarly to **A** but with 0.103 ± 0.002% Na^+ and no detectable K^+; this corresponds to $(Na_{0.020}H_{0.980})Fe_5O_8$.

On going from $Fe_{3-x}O_{4-x}$ to maghemite, the attainable saturation magnetization (see below) increased by about 7%, but there was no significant change in the SSA.

In our hands, attempts to prepare maghemite by the method of Rao *et al.* (37) involving thermal decomposition of $FeC_2O_4 \cdot 2H_2O$ gave products which contained 50–80% α-Fe_2O_3 (XRD) and up to 1.7% iron(II), as well as maghemite.

Kinetics of the Hydrothermal Conversion of Maghemite to α-Fe_2O_3

Typically, 0.500 ± 0.003 g maghemite was mixed with water or aqueous alkali[2] (usually 5.0 or 10.0 cm^3) in PTFE-lined autoclaves (small capacity of stainless steel (38), larger of titanium (35)), sealed under nitrogen or air as required, and thermostatted to ±0.2 K in a preheated forced-convection oven (38). The autoclaves were withdrawn and quenched in cold water after selected times t_{oven} in the furnace; the effective reaction time t_{corr} was taken to be $t_{oven} - 0.7$ h, as previously established and verified by extrapolation in those cases exhibiting "first order" kinetics (see below). The solid contents were filtered, washed with water and then acetone, then air-dried.

The percentage of maghemite in these products was estimated from the apparent percentage weight increase Δw experienced by small samples in a Faraday magnetic susceptibility apparatus (cf. ref. 39) under conditions of linear dependence of Δw on applied field, i.e., of saturation magnetization. Calibration with $HgCo(NCS)_4$ indicated the product of field and field gradient, held constant according to a gaussmeter for all samples in a given kinetic run, to be typically about 3×10^3 g cm^{-2} s^{-2}, giving Δw of about 26% for freshly-prepared maghemite, as against 0.03% for the feebly ferromagnetic product, α-Fe_2O_3. It was established, using prepared mixtures of maghemite and α-Fe_2O_3, that Δw was essentially proportional (±2%) to the percentage of maghemite, once this had been equilibrated with the hydrothermal medium (see below). The magnetization of hydrothermally-treated maghemite just before the onset of conversion to hematite in a kinetic run was taken to represent 100% maghemite; in most cases, the Δw value for $t_{oven} = 0.5$ h sufficed.

Results

(*i*) The aerial oxidation of magnetite to maghemite proceeded more rapidly in the "dry" state than under hydrothermal conditions. The oxidation of $Fe_{3-x}O_{4-x}$ (SSA ~ 75 m^2 g^{-1}) at 180°C was complete in 15 min without change in SSA (cf. refs. 14 and 40), and the product remained unchanged over a further 72 h at this temperature, whether prepared with exclusion of silica or not. By contrast, oxidation of $Fe_{3-x}O_{4-x}$ by excess air under hydrothermal conditions (1.0 *M* alkali or neutral) at 180°C was incomplete after several hours, in which time conversion of maghemite to α-Fe_2O_3 would have been important (e.g., 99% complete in 12 h in water, if silica-free).

(*ii*) Coarsely-crystalline, stoichiometric Fe_3O_4 underwent "dry" oxidation in (moist) air slowly and directly to α-Fe_2O_3, whereas finely-particulate $Fe_{3-x}O_{4-x}$ oxidized rapidly to maghemite first. Well-crystallized magnetite (SSA < 0.1 m^2 g^{-1}, particle size 10–100 μm (36)) gave only 2% α-Fe_2O_3 after 24 h at 260°C, according to chemical analysis and XRD; the small-angle reflections characteristic of maghemite were entirely absent. Under these conditions, a sample of genuine maghemite (SSA 72 m^2 g^{-1}) decomposed only to the extent of 5% α-Fe_2O_3; at 400°C, 50% α-Fe_2O_3 resulted after 24 h, and 95% after 4 days. Thus, had maghemite been the initial product of oxidation of the well-crystallized Fe_3O_4 at 260°C, it would surely have been detected.

(*iii*) Freshly-prepared silica-free maghemite picked up moisture from the air, reaching constant weight within a few hours. This material contained significant amounts of alkali metal ion M^+ from the MOH used in making $Fe_{3-x}O_{4-x}$, despite washing this last until the filtrate was neutral, and analyzed as $(H_{1-\delta}M_\delta)Fe_5O_8$, within experimental uncertainty, with δ typically 0.02 (material **B**, M = Na) to 0.03 (material **A**, M = K). Hydrothermal treatment at ~ 175°C in pure water decreased the M^+ content slightly, e.g., from 0.28 to 0.22% K in **A**, before decomposition to α-Fe_2O_3 was detectable, and this was accompanied by an increase of ~5% in the apparent SSA (measured *after drying* at 180°C; see Table 1) as well as an increase of 11–13% in the saturation magnetization attainable in the Faraday measurements. Samples of $Fe_{3-x}O_{4-x}$ also showed an augmentation in the attainable saturation magnetization on hydrothermal treatment, the increase being roughly proportional to x.

Treatment of $H_{1-\delta}M_\delta Fe_5O_8$ with aqueous MOH (0.1–1.0 *M*) at ~175°C, on the other hand, increased δ markedly (e.g., from 0.28 to 0.82% K^+ for **A** in 1.0 *M* KOH) before detectable α-Fe_2O_3 formation, and the attainable saturation magnetization *decreased* by 7% (0.1 *M* KOH) to 12% (1.0 *M* KOH) simultaneously. Treatment of $H_{1-\delta}M_\delta Fe_5O_8$ with aqueous M′OH at ~ 175°C led to the replacement of most of the M by M′, as well as an overall increase in the alkali metal ion content; thus, after $t_{oven} = 0.5$ h with the oven at 175°C, the K^+ content of substance **A** in 1 *M* NaOH fell from 0.28 to 0.047%, while the Na^+ content rose from < 0.005% to 0.32%.

The amount of moisture driven off from $H_{1-\delta}M_\delta Fe_5O_8$ at 180°C under dry nitrogen was close to that released on total decomposition to α-Fe_2O_3 in air at 800°C (2.1%), especially when δ was relatively large (Table 1), suggesting that small residual amounts of H^+ *or* M^+ are intricately involved in maintaining the spinel structure (cf. refs. 24, 25). Larger percentages of moisture (to ~5% for SSA ~ 120 m^2 g^{-1}) were recovered at 180°C from hydrothermally-treated maghemite which had been prepared using glassware; these percentages correlated roughly with surface area, and probably reflected contamination by silica.

(*iv*) The presence of silica retarded the hydrothermal decomposition of maghemite. Maghemite, made from $Fe_{3-x}O_{4-x}$ prepared with ~1.5 h exposure to boiling KOH in Pyrex glassware, was only 7% converted to α-Fe_2O_3 after 3 h in water at 187°C, whereas for silica-free maghemite the conversion to hematite was over 97% complete under

---

[2] Throughout this paper, concentration data refer to the original solutions at 294 K and 89 kPa, rather than hydrothermal conditions. Increases in concentration due to the generation of the saturated vapor pressure were in no case more than 0.3%.

TABLE 1. Correlation between the extent of hydrothermal conversion of silica-free maghemite (material A) to hematite and the specific surface and adsorbed moisture of the solid phases

T (°C)	Medium	t_{oven} (h)	% maghemite[a]	Specific surface[b] ($m^2\ g^{-1}$)	Water loss, 180°C ($mg\ g^{-1}$)
170.6	Water	2.0	100	74	
		4.0	98	70	
		6.0	90	69	
		8.0	76	59	
		10.0	58	43	
		13.5	27	22	
		16.0	12	12	
		22.0	1.5	5	
		28.0	0.4	3	
174.2	1.0 *M* KOH	0.5	100	75	20
		1.0	94	75	22
		2.0	92	75	22
		3.0	80	66	20
		5.0	62	51	14
		7.0	44	37	10
		9.0	28	24	8
		12.0	19	14	5
		17.8	5	4	1
		22.0	2	< 1	< 1
179.1	Water	0.5	100	74	16
		0.8	100	73	15
		1.0	100	73	17
		2.0	100	74	18
		3.0	94	72	18
		4.0	83	65	15
		6.0	60	46	9
		8.0	21	20	4
		12.0	2.3	$\lesssim 2$	—

[a] Experimental Δw values.
[b] Originally 71.5 $m^2\ g^{-1}$.

TABLE 2. Effect of contaminants on the extent of hydrothermal decomposition of maghemite at 174.8°C

Preparation of maghemite	Reaction medium	Time t_{oven} (h)	% maghemite remaining	Added solids per g maghemite	Specific surface ($m^2\ g^{-1}$)	
					Initial	After t_{oven}
Glassware	Water	21	100	—	118	113
		91	96	—		116
Silica-free	Water	19	< 0.1[a]	—	75	~ 2[b]
	1.0 *M* KOH	19	2	—		$\lesssim 0.1$
			93	20 mg SiO_2		49
			94	20 mg SiO_2+ 20 mg α-Fe_2O_3		74

[a] Calculated from data in Table 3.
[b] Typical value.

the same conditions. Table 2 gives data which confirm this effect and show unambiguously that the deliberate introduction of reagent-grade SiO_2 into the maghemite–hematite reaction mixture had similar results.

(*v*) The *nature* of the hydrothermal decomposition products of maghemite, also, depended to some extent upon the presence or absence of silica and the composition and temperature of the reaction medium. Silica-free maghemite was converted exclusively to α-Fe_2O_3 in both plain water and 1.0 *M* KOH or NaOH at all temperatures (150–190°C). Hematite was again the sole product in plain water when maghemite prepared in glassware was used, but in strongly alkaline solutions α-FeO(OH) (goethite) was also formed, and was the exclusive product in 1 *M* NaOH at 150–166°C. The product distribution was then also sensitive to the cation present; after 116 h at 174.8°C in 1 *M* MOH, maghemite prepared in glassware decomposed to the extent of 59% giving α-Fe_2O_3 and a trace of α-FeO(OH) when M was Na, and 90% giving α-FeO(OH) and a trace of α-Fe_2O_3 when M was K (silica-free maghemite decomposed to α-Fe_2O_3 completely and exclusively in all control experiments).

(*vi*) Neither the original maghemite nor its decomposition product, hematite, showed any decreases in surface area on hydrothermal treatment in water or 1 *M* NaOH that could be attributed to a significant degree of Ostwald ripening (crystal growth by dissolution and reprecipitation of the same phase) on the time-scale of the hydrothermal kinetic experiments, according to BET–SSA measurements and the scanning electron microscope (SEM). Thus, the decline in SSA accompanying the disappearance of maghemite, exemplified in Table 1, was a direct consequence of reaction to form relatively large crystals of hematite, growth of which effectively ceased on depletion of the maghemite nutrient. The small *increase* noted above in the apparent SSA of maghemite on initial exposure to hydrothermal environments probably reflected surface roughening by hydration followed by drying at 180°C in the BET procedure.

The final product in plain water was red hematite of SSA about 2 $m^2 g^{-1}$ (cf. 40–120 $m^2 g^{-1}$ for the original maghemite); a sample of SSA 5 $m^2 g^{-1}$ in which 4% unreacted maghemite remained was seen under the SEM to consist mainly of α-Fe_2O_3 rhombohedra of size 0.3 μm in general and in no case greater than 1.0 μm. In 1.0 *M* KOH, the hematite product was purple–brown to metallic grey, the SSA was not measurable ($\lesssim$ 0.1 $m^2 g^{-1}$) with the apparatus available, and the SEM showed it to consist mainly of well-crystallized tables up to 5 μm across and about 1 μm thick, morphologically similar to the larger hematite crystals prepared hydrothermally by Laudise and co-workers (41).

Maghemite (substance **A**, 72 $m^2 g^{-1}$), heated for 1 h at 800°C in air, decomposed to hematite of SSA 5 $m^2 g^{-1}$.

(*vii*) The decay curves of maghemite, defined by Δw, were sigmoidal in plain water but approached exponential at high alkali concentrations (Table 1 and Fig. 1). These curves can be generally represented to within the experimental uncertainty by the equation

$$[1] \quad -\ln(1-\alpha) = (kt_{\mathrm{corr}})^n$$

where α is the molar fractional extent of reaction at the effective reaction time t_{corr} (so that % maghemite = $100(1-\alpha)$), n is a constant determining curve shape (exponential if $n = 1$, sigmoidal if $n > 1$), and k is a time-scaling constant. Equation [1] resembles those developed by Avrami (42), Erofeyev (43), and others (44, 45) for phase transformations in homogeneous solids, but similar equations describe some chemical dissolution processes involving metal oxides (46) and, indeed, a variety of non-chemical phenomena (Weibull–Kao statistics) (47, 48). We emphasize that our choice of eq. [1] was made on purely empirical grounds, without reference to any mechanistic model, and accordingly no special interpretation should be attached to the shape and scaling parameters, n and k.

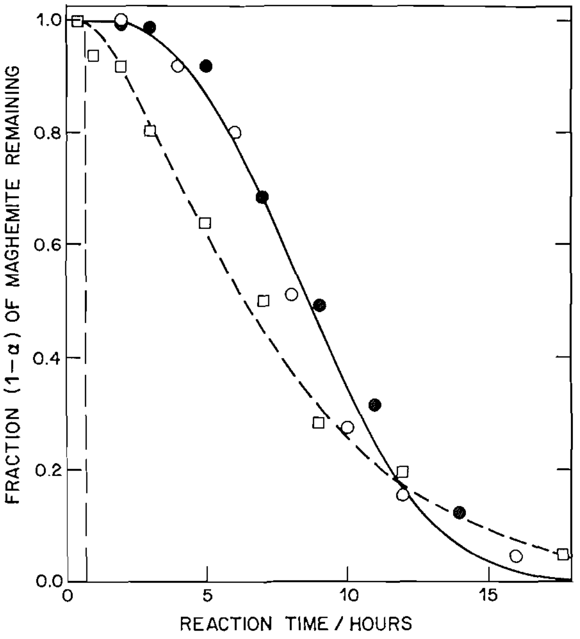

FIG. 1. Hydrothermal conversion of silica-free maghemite (preparation **A**) to hematite at 174.5 ± 0.3°C. Open circles: plain water. Filled circles: plain water, 20 mg α-Fe_2O_3 per g maghemite added. Squares: 1.05 *M* KOH. Vertical broken line: effective zero reaction time. Curves: fit of data to eq. [1].

Table 3 summarizes the kinetics of the hydrothermal transformation of silica-free maghemite to hematite according to eq. [1], based on Δw measurements; SSA and moisture content data (Table 1) and estimates of the relative amounts of maghemite and hematite by XRD were less precise than Δw, but confirmed these results semi-quantitatively at least. These reaction rates were independent of the age of the maghemite sample (up to 1 year), the presence of O_2 or CO_2 in the autoclaves, the nature of M^+ in the MOH used in the preparation and in the reaction mixture, the relative amounts of the solid and liquid phases (the latter was always at least 10-fold greater by weight), and the dimensions and structural metal of the autoclaves. After comple-

TABLE 3. Representation of the kinetics of the hydrothermal conversion of silica-free maghemite (material **A**) to hematite in terms of eq. [1][a]

[KOH] (M)	T (°C)	M	10^5k (s^{-1})	r (no. of data)
None	187.2	2.24 ± 0.18	20.2 ± 1.4	0.982(8)
	179.1	2.59 ± 0.12	4.2 ± 0.3	0.997(5)
	174.7	2.64 ± 0.17	3.1 ± 0.4	0.992(7)
	170.6	2.80 ± 0.08	2.33 ± 0.15	0.998(7)
	160.6	2.45 ± 0.10	1.36 ± 0.16	0.998(7)
1.0×10^{-3}	174.3	2.40 ± 0.24	2.7 ± 0.6	0.986(5)
1.0×10^{-2}	174.7	2.37 ± 0.16	5.7 ± 0.7	0.991(6)
1.0×10^{-1}	174.3	1.70 ± 0.07	3.1 ± 0.3	0.993(9)
1.0	174.2	1.35 ± 0.03	3.8 ± 0.2	0.999(8)
1.0×10^{-1}	187.2	1.34 ± 0.06	8.9 ± 0.4	0.997(4)
1.0	187.2	1.69 ± 0.09	9.7 ± 0.5	0.997(4)

[a] From magnetization (Δw) data; r is the coefficient of correlation, and ± indicates standard deviation. Specific surface of starting material 72 m^2 g^{-1} in all cases.

TABLE 4. Effect of initial surface area A_0 on the kinetics of hydrothermal conversion of silica-free maghemite to hematite in water at 187.5°C

t_{oven} (h)	% γ observed ($A_0 = 46$ m^2 g^{-1})	% γ calculated[a] ($A_0 = 75$ m^2 g^{-1})
0.5	100	100
1.0	90	97
2.0	53	42
2.5	28	16
3.0	11	4

[a] Interpolated from data of Table 2.

tion of the reactions in plain water, the liquid phase was neutral or slightly alkaline.

Early experiments using maghemite prepared in glassware showed, in general, a similar conformity to eq. [1], e.g., at 178°C, $n = 1.8$ with $k = 4.3 \times 10^{-5}$ s^{-1} for 0.01 M NaOH, and $n = 1.0$ with $k = 2.7 \times 10^{-5}$ s^{-1} for 0.10 M NaOH, confirming the general effect of $[OH^-]$ upon n seen in Table 3; the possibility of silica contamination, however, excludes these data from the table.

(*viii*) "Seeding" the reaction mixture with α-Fe_2O_3 up to the same amount as maghemite did *not* accelerate the conversion of maghemite to hematite, regardless of the presence or absence of alkali or of silica (Table 2 and Fig. 1). An apparent slight *retarding* effect of added hematite is too small to be significant.

(*ix*) The rate of the hydrothermal conversion of maghemite to hematite was somewhat greater the larger the SSA of the starting material (A_0), as Table 4 shows for silica-free maghemite in water. These data, on fitting to eq. [1] with n fixed at 2.24, give $k = 1.7 \times 10^{-4}$ s^{-1} for $A_0 = 46$ m^2 g^{-1} and $k = 2.0 \times 10^{-4}$ s^{-1} for $A_0 = 75$ m^2 g^{-1}. In an early experiment, good fits to eq. [1] were obtained with $n = 1.00$ (cf. "first order" homogeneous reaction kinetics) for maghemite samples of $A_0 = 85$ and 120 m^2 g^{-1} in 0.1 M NaOH at 178°C, giving $k = 2.7 \times 10^{-5}$ and 6.4×10^{-5} s^{-1} respectively; these samples were, however, prepared using glassware. The important point is that the effect of SSA was quite small below, say, 80 m^2 g^{-1}, so that it was possible to obtain reproducible kinetics from one batch of maghemite to another so long as the SSA's were roughly similar.

(*x*) "Maghemite" made from ferrous oxalate (37) had a relatively low SSA (32 m^2 g^{-1}) yet showed a rapid decline in Δw on hydrothermal treatment, e.g., even at 95°C, $k \sim 4 \times 10^{-5}$ s^{-1} with $n \sim 1.0$ in eq. [1]. This material, however, contained 0.7% iron(II) in addition to some 50% α-Fe_2O_3; since the latter has been shown not to affect the hydrothermal conversion rate of pure maghemite to hematite, it appears that iron(II) may catalyze the reaction. For all other maghemite preparations used in these kinetic studies, however, the iron(II) content was known to be much less than 0.01% and was probably less than 0.001%.

Discussion

The analytical data and the observations (*iii*) support the suggestion of Braun (24) that maghemite, as prepared and used in this study, is better represented as HFe_5O_8, rather than in the traditional way as "γ-Fe_2O_3", but they also show that the protons which fill the octahedral cation vacancies of the pseudo-spinel Fe_2O_3 structure (24, 25) are to some extent exchangeable with Na^+ and K^+. These respective ions will therefore be present in maghemite derived from magnetite prepared by precipitation of iron(II)–(III) mixtures with hot aqueous NaOH or KOH, since this magnetite is not stoichiometric Fe_3O_4 but rather a solid solution of Fe_3O_4 in maghemite, represented above as $Fe_{3-x}O_{4-x}$ but in fact containing moisture (and hence protons in cation sites) roughly in proportion to x. Alkali-metal ferrites with the spinel ($LiFe_5O_8$, $NaFe_5O_8$) (24, 49) or other (KFe_5O_8) (49, 50) structures, or of the "β-alumina" type $(1 + y)M_2O \cdot 11Fe_2O_3$ (M = Na, K) which retains some elements of the spinel structure (51–56), are well known, as are some mixed-alkali-metal analogues (51, 57). The maghemite samples $H_{1-\delta}M_\delta Fe_5O_8$ prepared in this study contained far less alkali metal ion than these ferrites, since δ was always less than 0.1, but we note that the saturation magnetization of maghemite decreased as δ increased, in accordance with the lack of ferromagnetism at room temperature in ferrites such as KFe_5O_8, KFe_7O_{11}, and $KFe_{11}O_{17}$ (50, 52).

The mechanism of oxidation of "dry" magnetite by air has been the subject of controversy (9–13), but it seems that the presence of water is necessary for maghemite production, otherwise hematite is formed (9, 11, 22–25). This applies whether or not α-Fe_2O_3 nuclei are present (13, 23). The present study (results (*iii*)) suggests that uptake of water from the gas phase by magnetite is associated with non-stoichiometry in the latter ($Fe_{3-x}O_{4-x}$, $0 < x \leq 1$), presumably because the protons of the water can be accommodated in the cation vacancies, concomitantly stabilizing the spinel structure (22–25, 58); thus, coarsely crystalline, *stoichiometric* Fe_3O_4 oxidizes to α-Fe_2O_3 even when prepared by a "wet" method (36) (results (*ii*)). Since the finely-particulate magnetite which results from conventional "wet" methods is invariably non-stoichiometric, and indeed since surface oxidation of any very finely powdered magnetite can lead to significant overall departures from stoichiometry, the well-established correlation (9–15) between magnetite particle size and oxidation product can be recast in terms of the capacity of the non-stoichiometric solid for water uptake.

The oxidation of magnetite evidently involves the migration of Fe^{3+} ions outwards toward newly-formed O^{2-} at the crystal surface (40). The oxidation should therefore proceed relatively quickly to maghemite if sufficient water protons are present to preserve the spinel structure during oxidation, but *not* so many as to *eliminate* the cation vacancies, through which the Fe^{3+} ions can diffuse with relative ease. If this picture is correct, the aerial oxidation of $Fe_{3-x}O_{4-x}$ in hydrothermal conditions should still yield maghemite, but at a much *slower rate* than in air alone, because cation vacancies will be almost immediately eliminated by the large excess of water. This is indeed the case (result (*i*)); thus, paradoxically, although water is necessary for the production of maghemite, a superabundance of water suppresses the rate of the process dramatically.

A further paradox is that the presence of liquid water accelerates the subsequent decomposition of maghemite to hematite, despite the importance of water in enabling maghemite to exist.

The hydrothermal decomposition of maghemite occurs in a temperature regime some 170°C cooler than does the "dry" transformation to hematite, as may be seen by comparing Tables 1 and 2 with Feitknecht and Mannweiler's Fig. 2 (59) (which refers to a maghemite preparation "1" closely similar in particle size to our preparations **A** and **B**). The SEM showed that the reaction in plain water gave nicely-formed rhombohedra of α-Fe_2O_3, much larger (~300 nm length) and better shaped than either the parent maghemite crystals or hematite formed by the decomposition of the dry solid in air at higher temperatures, as exemplified by Feitknecht and Mannweiler's Fig. 6 (59). Thus, although increases in crystallite size and decreases in SSA are observed in the conversion of "dry" maghemite to hematite as well as in the hydrothermal reaction, the mechanisms of reaction are evidently different, a topotactic particle-to-particle chain reaction being likely in the former (59) and a dissolution–reprecipitation process involving discrete particles in the latter. Alkaline hydrothermal media produced still larger, clean-facetted tables of hematite, characteristic of growth from hydrothermal solution (41).

The kinetics of the hydrothermal decomposition of maghemite in plain water (results (*vii*)) differed from those of the "dry" reaction in being much faster and in the sigmoidal, as opposed to roughly exponential, shape of the plots of extent of reaction vs. time (Fig. 1, compare refs. 58 and 59). Again, markedly different reaction mechanisms are indicated. The Avrami–Erofeyev type of relationship (eq. [1]), which describes the sigmoidal curves, empirically, is commonly associated with reactions occurring in initially homogeneous solid phases (42–45), although Kabai (46) applied it to the kinetics of dissolution of metal oxides in aqueous acids with the conclusion that values of *n* greater than unity were associated with physical disintegration of the solid oxide (increase in SSA); neither situation, however, seems relevant in the present context.

The observation (*viii*), that seeding with α-Fe_2O_3 does *not* accelerate the hydrothermal transformation of maghemite, eliminates hematite nucleation and the availability of hematite surfaces for growth as rate-determining factors. Furthermore, the absence of any evidence for hydrothermal ripening of either maghemite or hematite on the time-scale of these kinetic experiments (results (*vi*)) argues against any rapid dissolution–reprecipitation pre-equilibrium, or reversibility of the precipitation of α-Fe_2O_3, as mechanistically significant processes. The most feasible remaining mechanistic model, therefore, is one in which both the dissolution of maghemite and a subsequent solution-phase step leading to the precipitation of α-Fe_2O_3 are slow and irreversible. The latter process may require a pre-existing α-Fe_2O_3 surface or surrogate, but the *extent* of this may not be rate determining if the concentration of iron(III) in solution is very low (as seems likely). Reactions [2] and [3] seem reasonable models; the aqueous form of iron(III) is taken to be the neutral hydroxo-species in accordance with the predominance of cation hydrolysis under hydrothermal conditions (35) and the absence of any significant effect of low concentrations of alkali.

[2] $2HFe_5O_8(s) + 14H_2O(l) \rightarrow 10Fe(OH)_3(aq)$

[3] $10Fe(OH)_3(aq) \rightarrow 5\alpha\text{-}Fe_2O_3(s) + 15H_2O(l)$

Taking reaction [3] to be first-order in iron(III) its rate will be limited at first by the slow build-up of $[Fe(OH)_3]$ from zero; then, after a relatively rapid main phase, the diminished surface of maghemite remaining will limit the dissolution rate (we note that SSA does affect the reaction rate somewhat — observation (*ix*)), leading to a sigmoidal plot of α against time. Assuming, by analogy with $Ni(OH)_3^-(aq)$ (32), that $Fe(OH)_4^-(aq)$ becomes the important iron(III) species in water at high pH and elevated temperatures, we can anticipate that high $[OH^-]$ will speed up the supply of iron(III) to the solution phase but, by the same token, slow the precipitation step by permitting higher [Fe(III)] to remain in solution. This will lead to an approach to exponential kinetics ($n = 1$ in eq. [1]) which are faster than the corresponding sigmoidal kinetics in the earlier stages but slower later; this is indeed observed (Fig. 1), and the larger, better-formed $\alpha\text{-}Fe_2O_3$ crystals obtained in 1 *M* alkali also suggest higher iron(III) levels in solution and slower precipitation.

[4] $2HFe_5O_8(s) + 10OH^-(aq) + 14H_2O(l) \rightleftharpoons 10Fe(OH)_4^-(aq)$

[5] $10Fe(OH)_4^-(aq) \rightarrow 5\alpha\text{-}Fe_2O_3(s) + 10OH^-(aq) + 15H_2O(l)$

Since maghemite exhibits ion-exchanging properties, the solid that reacts in aqueous KOH is not, strictly speaking, chemically the same as that in aqueous NaOH or in plain water. Fortunately, the rate of formation of hematite from maghemite was found to be the same in 1 *M* NaOH as in 1 *M* KOH, so that it is permissible to write eqs. [4] and [5] simply in terms of HFe_5O_8 and OH^-.

The above facts and proposed mechanisms contrast with those for the superficially similar alkaline hydrothermal conversion of $Ni(OH)_2$ to NiO (32), in which the reaction corresponding to [4] is rapid and reversible (giving rise to Ostwald ripening of $Ni(OH)_2$), the rate of the step analogous to [5] is completely controlled by the available area of NiO (leading to a dependence of α on $t_{corr}{}^3$), and neutral-pH pathways analogous to [2] and [3] are undetectable.

The dramatic retardation of the hydrothermal decomposition of maghemite by silica (results (*iv*), (*v*)) has obvious implications relating to the survival of maghemite in nature, where it is usually accompanied by quartz (2), and to laboratory practice in investigating iron oxides. Any explanation of the effect needs to accommodate the facts that, when silica is present and the pH is high, goethite may form in place of hematite when the alkali cation present in solution is K^+ but is itself suppressed, leaving hematite as the major product in the long term, when the cation is Na^+. Four distinct modes of involvement of silica can readily be visualized, but each presents problems.

(*a*) Iron(III) becomes complexed by silicate species in solution, so retarding steps [3] and [5]. Thermodynamic data on the weak complexing of Fe^{3+} by $Si(OH)_4$ at 25°C and low pH are available (60) but are inapplicable to high temperatures and neutral or alkaline solutions because of hydrolysis and polymerization. Even if the complexing power of low levels of dissolved silicate could be shown to be sufficient to reduce the iron(III) concentration markedly, however, this alone would not explain why goethite may form instead of hematite in some circumstances but not in others. Many polybasic anions (61) including silicate (62, 63) are known to inhibit the somewhat analogous aqueous conversion of iron(III) hydroxide gels to $\alpha\text{-}FeO(OH)$, but there is no correlation of this effect with iron(III) complex stability constants, again suggesting that inhibition by such potential complexing agents occurs elsewhere than in the solution phase.

(*b*) Silica impregnates or coats the maghemite with a dissolution-resistant iron(III) silicate, so suppressing steps [2] and [4]. Chemisorption of this kind has been demonstrated for other iron(III) oxide – hydroxide materials by infrared spectroscopy, although, just as in the present study, XRD patterns gave no indication of this (17, 63). Highly resistant coatings of acmite, $NaFeSi_2O_6$, form readily in hydrothermal media containing NaOH, iron(III), and silica, but no potassium analogue is known (64); this suggests a connection with the fact that goethite formation, though favored by high concentrations of KOH (cf. decomposition of ferrihydrite (65)), is itself suppressed by NaOH. It is, however, difficult to see why the identity of the final product should be determined by suppression of step [4] rather than by influencing [5]; goethite was never obtained when silica was absent.

(*c*) Decomposition via dissolution is stopped by silica as in (*b*), but slow solid-phase reactions continue (cf. Schwertmann (61)). Neither direct measurement (results (*i*)) nor extrapolation of rate data (58, 59) indicate any significant solid-state decomposition of maghemite at ~180°C on the time-scale of our experiments, but it is conceded that "dry" decompositions involve a different (partially dehydrated) kind of maghemite from that present in the hydrothermal systems.

(*d*) Silica eliminates the nuclei or coats the growth surfaces of the product, possibly by acmite formation. Such an interaction would presumably affect goethite differently from the less reactive hematite, and would also explain the cation effect as in (*b*). Unfortunately, the evidence of seeding experiments (results (*viii*), Fig. 1, and Table 2) indicated in every case that nucleation and product surface availability were *not* rate-controlling in hematite formation, although they might have been in the production of goethite (65, 66). The possibility remains that these factors may come to be rate-controlling if they are drastically reduced by interaction with silica; a small quantity of silica could conceivably deactivate large areas of product growth surface or large numbers of nuclei.

Some light may be shed on this mechanistic problem by comparing the characteristics of the hydrothermal transformation of maghemite ("γ-Fe_2O_3") with those reported by Schwertmann and Taylor (66) for the conversion of lepidocrocite (γ-FeO(OH)) to goethite in aqueous alkali at 20–80°C. In common with the Fe_2O_3 system, the FeO(OH) conversion occurs via solution rather than topotactically, is faster for smaller particles, follows various kinds of rate equations (including sigmoidal and quasi-exponential) depending on [KOH] and temperature, and is suppressed by silicate. On the other hand, the Ostwald ripening of FeO(OH) in the presence of silicate, the marked accelerating effect of KOH, and the facilitation of reaction by seeding differentiate the FeO(OH) system from the Fe_2O_3. Schwertmann and Taylor (66) argue persuasively that silicate affects the γ-FeO(OH) reaction by inhibiting nucleation of goethite. We therefore suggest that silica together with Na^+ affects the production of goethite from maghemite by suppressing its nucleation, but that silica affects the more important reaction, α-Fe_2O_3 formation, through some other process, probably similar to (*b*) above.

Finally, we note that agitation had no significant effect on the rate of reaction of γ-FeO(OH) (66). The same was taken to be true of the maghemite reaction, since diffusional processes are rapid in hydrothermal systems, but we were unable to check this assumption for lack of PTFE-lined, non-magnetic stirred autoclaves with precise temperature control.

Acknowledgements

We thank Dr. A. E. Oldershaw for SEM photographs, Mrs. D. Johnson for XRD patterns, Drs. P. Bayliss and H. L. Yeager for technical advice, and the Natural Sciences and Engineering Research Council of Canada for financial assistance.

1. U. Schwertmann. Fortschr. Miner. **46**, 274 (1968).
2. R. M. Taylor and U. Schwertmann. Clay Miner. **10**, 289 (1974).
3. E. I. Nikitina, V. I. Sotnikov, A. A. Proskuryakov, D. K. Archipenko, and L. M. Krivoputskaya. Miner. Paragenezisy Miner. Gidroterm. Mestorozhd. 61 (1974); Chem. Abstr. **83**, 100844 (1975).
4. P. Toulmin III, A. K. Baird, B. C. Clark III, K. Keil, H. R. Rose, Jr., R. P. Christian, P. H. Evans, and W. C. Kelliher. J. Geophys. Res. **82**, 4625 (1977).
5. A. O. Fuller and R. B. Hargreaves. Icarus, **34**, 614 (1978).
6. D. R. Huffmann. Astrophys. J. **161**, 1157 (1970).
7. P. G. Manning. Chem. Soc. Rev. **5**, 233 (1976).
8. E. Z. Basta. Econ. Geol. **54**, 698 (1959).
9. W. Feitknecht and H. W. Lehmann. Helv. Chim. Acta, **42**, 2035 (1959).
10. U. Colombo, F. Gazzarrini, G. Lanzavecchia, and G. Sironi. Science, **147**, 1033 (1965).
11. T. Elder. J. Appl. Phys. **36**, 1012 (1965).
12. K. J. Gallagher, W. Feitknecht, and U. Mannweiler. Nature, **217**, 1118 (1968).
13. W. Feitknecht and K. J. Gallagher. Nature, **228**, 548 (1970).
14. K. Haneda and A. H. Morrish. J. Phys. **38**, Cl-321 (1977).
15. B. Gillot, A. Rousset, and G. Dupre. J. Solid State Chem. **25**, 263 (1978).
16. R. M. Taylor and U. Schwertmann. Clay Miner. **10**, 299 (1974).
17. U. Schwertmann and H. Thalmann. Clay Miner. **11**, 189 (1976).
18. V. I. Bagin. Izv. Akad. Nauk S.S.S.R., Fiz. Zemli, 104 (1967); Chem. Abstr. **67**, 48439k (1967).
19. J. D. Bernal, D. R. Dasgupta, and A. L. MacKay. Nature, **180**, 645 (1957).
20. R. Giovanoli and R. Brütsch. Thermochim. Acta, **13**, 15 (1975).
21. H. W. Van Der Marel. J. Sedimentol. Petrol. **21**, 12 (1951).
22. I. David and A. J. E. Welch. Trans. Faraday Soc. **52**, 1642 (1956).
23. H. P. Johnson and R. T. Merrill. J. Geophys. Res. **77**, 334 (1972).
24. P. B. Braun. Nature, **170**, 1123 (1952).
25. A. Aharoni, E. H. Frei, and M. Schieber. J. Phys. Chem. Solids, **23**, 545 (1962).
26. M. A. Gheith. Am. J. Sci. **250**, 677 (1952).
27. J. L. Kulp and A. F. Trites. Am. Miner. **36**, 23 (1951).
28. M. Nagayama and M. Cohen. J. Electrochem. Soc. **109**, 781 (1962); **110**, 670 (1963).
29. K. A. Nesmeyanova, V. I. Kasatkin, V. A. Gashenko, and V. G. Kasatkina. Teploenergetika (Moscow), 54 (1976); Chem. Abstr. **84**, 183175n (1976).
30. D. E. Davies and U. R. Evans. J. Chem. Soc. 4373 (1956).
31. U. R. Evans. The corrosion and oxidation of metals. First supplementary volume. Edward Arnold, Ltd., London. 1968. pp. 25, 26.
32. T. W. Swaddle and T. C. T. Wong. Can. J. Chem. **56**, 363 (1978).
33. A. I. Vogel. A textbook of quantitative inorganic analysis. 3rd ed. Longmans, London. 1961.

34. G. N. Schrauzer and T. D. Guth. J. Am. Chem. Soc. **98**, 3508 (1976).
35. T. W. Swaddle, J. H. Lipton, G. Guastalla, and P. Bayliss. Can. J. Chem. **49**, 2433 (1971).
36. M. Booy and T. W. Swaddle. Can. J. Chem. **56**, 402 (1978).
37. V. Rao, A. L. Shashimohan, and A. B. Biswas. J. Mater. Sci. **9**, 430 (1974).
38. M. Booy and T. W. Swaddle. Can. J. Chem. **55**, 1762 (1977).
39. N. A. Vasyutinskii. Izv. Akad. Nauk S.S.S.R. Met. Gorn. Delo, 39 (1963); Chem. Abstr. **59**, 12511e (1963).
40. P. S. Sidhu, R. J. Gilkes, and A. M. Posner. J. Inorg. Nucl. Chem. **39**, 1953 (1977).
41. E. D. Kolb, A. J. Caporaso, and R. A. Laudise. J. Cryst. Growth, **19**, 242 (1973).
42. M. Avrami. J. Chem. Phys. **7**, 1103 (1939); **8**, 212 (1940).
43. B. V. Erofeyev. Compt. Rend. Acad. Sci. U.R.S.S. **52**, 511 (1946).
44. D. Turnbull. Solid State Phys. **3**, 225 (1956).
45. A. R. Allnatt and P. W. M. Jacobs. Can. J. Chem. **46**, 111 (1968).
46. J. Kabai. Acta Chim. (Budapest), **78**, 57 (1973).
47. W. Weibull. J. Appl. Mech. **18**, 293 (1951).
48. J. H. K. Kao. Technometrics, **1**, 389 (1959).
49. E. Lichtner and G. Szalek. Z. Anorg. Allgem. Chem. **360**, 151 (1968).
50. C. J. M. Rooymans, C. Langereis, and J. A. Schulkes. Solid State Commun. **3**, 85 (1965).
51. K. O. Hever. J. Electrochem. Soc. **115**, 826 (1965).
52. W. L. Roth. U.S. Patent No. 3,284,359 (Nov. 8, 1966).
53. W. L. Roth and R. J. Romanczuk. J. Electrochem. Soc. **116**, 975 (1969).
54. B. C. H. Steele. MTP Intern. Rev. Sci., Inorg. Chem., Ser. 1, Vol. 10. Butterworths, London. 1972. pp. 137–139.
55. G. J. Dudley and B. C. H. Steele. J. Solid State Chem. **21**, 1 (1977); J. Mater. Sci. **13**, 1267 (1968).
56. G. C. Farrington and J. L. Briant. Science, **204**, 1371 (1979).
57. M. Lenglet. Rev. Chim. Miner. **5**, 1169 (1968).
58. F. E. DeBoer and P. W. Selwood. J. Am. Chem. Soc. **76**, 3365 (1954).
59. W. Feitknecht and U. Mannweiler. Helv. Chim. Acta, **50**, 571 (1967).
60. L. L. Olson and C. R. O'Melia. J. Inorg. Nucl. Chem. **35**, 1977 (1973).
61. U. Schwertmann. Geoderma, **3**, 207 (1969).
62. W. Schellmann. Chem. Erde, **20**, 104 (1959).
63. A. J. Herbillon and J. Tran Vinh An. J. Soil Sci. **20**, 233 (1969).
64. R. A. Laudise. Prog. Inorg. Chem. **3**, 1 (1962).
65. D. G. Lewis and U. Schwertmann. Clays Clay Miner. **27**, 195 (1979).
66. U. Schwertmann and R. M. Taylor. Clays Clay Miner. **20**, 150 (1972); **20**, 159 (1972).